



HHS Public Access

Author manuscript

Bone. Author manuscript; available in PMC 2022 May 01.

Published in final edited form as:

Bone. 2021 May ; 146: 115889. doi:10.1016/j.bone.2021.115889.

Limited Impacts of Thermoneutral Housing on Bone Morphology and Mechanical Properties in Growing Female Mice Exposed to External Loading and Raloxifene Treatment

Carli A. Tastad¹, Rachel Kohler¹, Joseph M. Wallace¹

¹Department of Biomedical Engineering, Indiana University-Purdue University at Indianapolis, Indianapolis, IN, USA

Abstract

Thermoregulation is an important factor that could have physiological consequences on pre-clinical research outcomes. Simply housing mice at thermoneutral temperature has been shown to prevent the well-established loss of cancellous bone that is typical in growing mice. In this study, active tissue formation was induced by non-invasive tibial loading in female mice and combined with raloxifene treatment to assess whether temperature could enhance their combined effects on bone morphology and mechanical properties. It was hypothesized that by removing the cold stress under which normal lab mice are housed, a metabolic boost would allow for further architectural and mechanical improvements in mice exposed to a combination of tibial loading and raloxifene. Ten-week old female C57BL/6J mice were treated with raloxifene, underwent tibial loading to a maximum tensile stress of 2050 μe , and were housed in thermoneutral conditions (32°C) for 6 weeks. We investigated bone morphology through microcomputed tomography (μCT), mechanical properties via four-point bending, and fracture toughness testing. Results confirmed previous work showing a combined effect of external loading and raloxifene which led to greater improvements in most properties than either individual treatment. Counter to the hypothesis, temperature had modest effects on body weight, overall bone size, and trabecular architecture, and most effects were detrimental. Thermoneutrality had no impact on mechanical integrity or fracture toughness. In most cases, the magnitude of temperature-based effects were less robust than either RAL treatment or loading.

Corresponding Author: Joseph M. Wallace, Ph.D., Department of Biomedical Engineering, Indiana University-Purdue University at Indianapolis, Indianapolis, IN, USA, jmwalla@iupui.edu, +1-317-274-2448.

Credit author statement

Carli Tastad: Conceptualization, Methodology, Validation, Formal Analysis, Investigation, Writing Original Draft, Writing – Review and Editing, Visualization,

Rachel Kohler: Formal Analysis, Writing – Review and Editing

Joseph Wallace: Conceptualization, Methodology, Validation, Formal Analysis, Investigation, Resources, Writing – Review and Editing, Visualization, Project Administration, Funding Acquisition

Publisher's Disclaimer: This is a PDF file of an unedited manuscript that has been accepted for publication. As a service to our customers we are providing this early version of the manuscript. The manuscript will undergo copyediting, typesetting, and review of the resulting proof before it is published in its final form. Please note that during the production process errors may be discovered which could affect the content, and all legal disclaimers that apply to the journal pertain.

Declarations of Interest: None

Keywords

Axial Compression; Computed Tomography; fracture toughness; SERM; adaptation

1. Introduction

Mice are the most commonly utilized animal model for pre-clinical biomedical research. One factor that is not often considered, but is becoming better appreciated, is that the thermal physiological characteristics of mice may impact seemingly unrelated characteristics or endpoints in these models. The thermoneutral zone (TNZ) is the range of temperatures across which resting metabolic rate of heat production is at equilibrium with the animal's evaporative heat loss to the surrounding environment. TNZ is determined by body size and weight, morphology, condition, and resting metabolic rate, and therefore, spans only 1–3 °C in mice due to the large surface-to-volume ratio and meager body insulation. The lower and upper critical temperatures for a laboratory mouse is 30 and 32 °C, respectively, outside of which the mouse must engage in heating or cooling adjustments that can be behavioral and/or physiological (thermogenesis – shivering/non-shivering). [1,2] Therefore, laboratory mice housed under standard temperatures are subject to mild cold stress which has been attributed to physiologic changes. Since metabolism in these mice is altered to compensate, it is possible that the response of mice to stimuli which requires further metabolic changes could be blunted. Previous studies have demonstrated that in growing mice, simply housing the mice in thermoneutral conditions can prevent the well-established loss of cancellous bone that occurs in the distal femur. This finding suggests that temperature plays a critical physiologic role in bone development and homeostasis. [3,4] Other work in osteoporotic mice showed a beneficial impact of thermoneutral housing on trabecular bone properties, but cortical bone morphology was not impacted. [5] These studies introduce a potentially important factor to consider when designing preclinical intervention or treatment studies in mice (e.g. drug treatment, mechanical stimulation). This is especially true when interventions have a proven anabolic effect on bone, as metabolic responses may be magnified when mice are no longer challenged by cold stress from standard housing conditions.

Raloxifene (RAL) is a non-steroidal benzothiophene derivative that inhibits bone resorption by reducing osteoclast activity and reduces the rate of bone loss by binding and signaling through estrogen receptors on osteoblasts. [6] The efficacy of RAL is well demonstrated, with a clinical reduction in fracture risk by 50% with only modest changes in remodeling and BMD. [7,8] The lack of robust mass-based improvements suggests that changes in mechanical integrity are potentially driven by changes in tissue quality. Although the exact mechanism by which RAL reduces fracture risk is unknown, pre-clinical studies have demonstrated the ability of RAL to improve material-level properties in bone independent of BMD. Exploration of the mechanism behind improved fracture resistance has shown that RAL binds to collagen through its hydroxyl groups and increases bone tissue hydration by increasing the bound water content at the collagen-mineral interface. [9,10,11] These data would suggest that RAL modifies bone matrix quality independent of BMD, thus improving

material-level properties of the bone and offering a unique opportunity to enhance bone fracture resistance in a cell-independent manner.

Osteocytes are mechanosensory cells that are able to detect changes in the bone mechanical environment and direct osteoclast and osteoblast cell activity. The Mechanostat explains that an anabolic response to loading in bone is threshold driven. When a load is applied, the osteocytes direct osteoblasts to form new bone. [12] This active bone formation can be induced clinically through with high-impact exercises such as running or jumping. [13,14,15] *In vivo* non-invasive mechanical loading of the murine tibia has become a common model of mechanical stimulation. Compressive tibial loading has been shown to be anabolic in cortical and cancellous regions across multiple ages and sexes of mice, often leading to robust new bone in trabecular and cortical bone sites. [16,17,18,19]

Current standards for care of lab mice often house those mice at room temperature (22 °C), below metabolic TNZ and affecting physiological properties being studied. This study is expanding upon previous work [20] in which RAL was administered during a period of active tissue formation (tibial loading) to evaluate cumulative mechanical impacts of the combined treatments. The premise was that treatment with RAL during a period of increased tissue formation may allow for additional mechanical enhancements by improving quality in this newly forming tissue prior to mineralization. [16,17,18] Given the modest impacts of RAL in combination with tibial loading that were observed in this previous work, the current study considers the addition of thermoneutral housing at 32°C in an attempt to boost or amplify the effects.

By removing the mild cold stress placed on the animals, it was hypothesized that housing mice in a thermoneutral condition would facilitate an additive effect on bone mechanics in mice undergoing combined tibial loading and RAL treatment. Female mice were chosen based on the clinical use of raloxifene in humans, and also because the mechanical impacts were less pronounced in females in the previous study. By housing mice within their TNZ, a metabolic boost was expected, allowing loading and RAL to enhance the mechanical properties in bone further than either factor alone and more so than at standard housing temperatures.

2. Materials and Methods

2.1 Animals and Treatment

All protocols and procedures were performed with prior approval from the Indiana University – Purdue University Indianapolis School of Science Institutional Animal Care and Use Committee (Protocol SC296R). Female C57BL/6J mice were purchased from Jackson Laboratory (Bar Harbor, ME) at 9 weeks of age and allowed one week to acclimate to the animal housing facility. Mice were randomly assigned into four weight-matched groups (n = 20 per group): Standard-Control (Standard-CON), Standard-RAL, Thermoneutral-CON, and Thermoneutral-RAL. Half of the mice (n=40) were housed in either standard room temperature (22°C) or thermoneutral temperature (32°C) conditions, starting at 10 weeks of age and continuing for 6 weeks. One group in each housing condition was injected subcutaneously with RAL (0.5 mg/kg; 5x/week) in a 10% hydroxyl-β-

cyclodextrin solution. This dosage was chosen based on previous research showing efficacy *in vivo*. [21,22,23] Mice were weighed weekly. Untreated controls were also included in each housing condition. [24] At 16 weeks of age, the mice were euthanized by CO₂ inhalation followed by cervical dislocation. Tibiae were harvested, stripped of soft tissue, length was measured with calipers, and then they were wrapped in saline-soaked gauze and stored at -20°C until needed.

2.2 In vivo Tibial Loading

Starting at 10 weeks of age, each mouse underwent compressive tibial loading 3x/week for 6 weeks. Prior to the start of loading, a strain calibration study was performed on five mice to determine the average force necessary to induce a tensile strain of 2050 μe on the anteromedial surface, a level shown to be osteogenic in mice of this age and sex. [25] Mice were anesthetized (2% Isoflurane) and their left limb cyclically loaded in compression, leaving the contralateral limb as an internal control. Each loading profile consisted of 2 cycles at 4 Hz to a maximum load of 11.2 N, followed by a 1-second rest at 2 N, repeated 110 times for a total of 220 compressive cycles per day.

2.3 Microcomputed Tomography (μCT) and Architectural Analysis

To determine the effects of housing, loading, and treatment on bone architecture, both tibiae from each mouse were scanned *ex vivo* (three bones at a time) using an isotropic voxel size of 10 μm (Skyscan 1172, Bruker). Bones were scanned through a 0.5 mm Al filter ($V = 60\text{kV}$, $I = 167\mu\text{A}$) with a 0.7-degree angle increment and two frames averaged. Images were reconstructed (nRecon) and rotated (Data Viewer) before calibrating to hydroxyapatite-mimicking phantoms (0.25 and 0.75 g/cm^3 Ca-HA). A 1 mm trabecular region of interest (ROI) was selected at the proximal metaphysis (extending distally from the most distal portion of the growth plate), and then quantified using CT Analyzer (CTAn). A 0.1 mm ROI was selected at approximately 37.5% length of the tibia, the approximate site of maximum tensile strain, then analyzed with a custom MATLAB (MathWorks, Inc. Natick, MA) script. [25,26,19]

2.4 Four-Point Bending Mechanical Testing to Failure

Both tibiae from twelve mice per group were randomly selected for four-point bend tests to failure (lower support span at 9 mm, upper loading span at 3 mm), with the medial surface in tension (TA Instruments ElectroForce 3200). The bones were loaded at a displacement control rate of 0.025 mm/s while the sample remained hydrated with phosphate buffered saline (PBS). Cross-sectional cortical properties at the center of the load span were obtained from μCT images as described above. These properties were used to map load-displacement data into stress-strain data using standard engineering equations as previously reported to estimate tissue level properties. [27] Two bones in the standard control group and one bone from the thermoneutral control group were removed from analysis due to abnormal mechanical curves caused by rotation during testing. Contralateral limbs were also removed from the analysis.

2.5 Fracture Toughness Testing

Both tibiae from the remaining eight mice from each group were used for fracture toughness testing using a linear elastic fracture mechanics approach. [28,29] A notch was made through the anteromedial surface of the tibia, at approximately 50% of the bone length, using a straight razor blade lubricated with a 1 μm diamond suspension. The tibiae were notched into the medullary cavity, not exceeding the bone's midpoint. One bone each from the standard and thermoneutral control groups was broken during notching and thus removed from analysis. Additionally, the contralateral limbs were not considered for analysis. The bones were then tested to failure in three-point bending at a displacement rate of 0.001 mm/s with the notched surface in tension and the notched site directly below the load point.

After mechanical testing, the bones were cleaned of marrow and dehydrated in an ethanol gradient (70–100%), then dried overnight in a vacuum desiccator. The proximal cross-sectional fracture surface of the dehydrated bones was sputter-coated with gold and then imaged with scanning electron microscopy (SEM, JEOL JSM-7800f). The SEM images revealed the angles of stable and unstable crack growth, which were used in conjunction with geometric properties from μCT data at the notch site to calculate the stress intensity factors for crack initiation, maximum load, and fracture instability, using a custom MATLAB script.

2.6 Statistical Analysis

Repeated measures (RM) three-way ANOVA tests were used to statistically analyze main effects of housing temperature, treatment, and loading. A two-way ANOVA test was used to statistically analyze main effects of housing and treatment for body weights. If a significant triple interaction occurred, the ANOVA was followed by a Tukey post-hoc test. If an interaction occurred between only two factors, the ANOVA was followed by a Sidak post-hoc test. Analysis was performed using GraphPad Prism (v.8) with a significance level at $\alpha = 0.05$. Cohen's D statistical effect sizes were calculated by dividing two population mean differences by their pooled standard deviation in order to quantify the strength of the differences between two groups. Effects sizes were calculated between RAL and CON in non-loaded animals to determine the effect size for RAL, between loaded and non-loaded in CON animals to determine the effect size for loading, and between loaded+RAL and non-loaded CON to determine the combined effect size. Each of these effect sizes were determined within the standard housing group and then again within the thermoneutral housing group. The effect size for temperature was also calculated between thermoneutral and standard housing in non-loaded, CON animals to determine the impact of thermoneutral housing alone.

3. Results

3.1 Body Weight and Tibial Length

At the beginning of the study, mice were placed in weight-matched groups. Each group increased weight throughout the duration of the study: standard-CON (+7.3%), standard-RAL (+3.2%), thermoneutral-CON (+3.9%), thermoneutral-RAL (+1.5%). At the study end,

thermoneutral housing temperature ($p=0.0196$) and RAL treatment ($p=0.004$) led to decreased body weight, but these differences were modest and significance was likely driven by the large sample sizes (Fig-1A). Tibial length was also significantly decreased due to RAL ($p=0.0306$), but increased due to loading ($p=0.0022$) (Fig-1B). These changes were also modest.

3.2 Cancellous Architecture Improves Due to Loading and RAL Treatment with Modest Impact from Temperature

Both loading and RAL improved trabecular architecture and mineralization in all properties investigated. Raloxifene significantly increased bone volume fraction (BV/TV, $p<0.0001$) (Fig-2A), but an interaction effect from loading x temperature was also present ($p=0.0074$). The increased effect due to loading is clear in all post-hoc analyses, but appears to be greater at thermoneutral temperatures as indicated by the numerically greater effect size at thermoneutral vs. standard temperature (Table 2). The effect due to RAL (effect size=1.837) was similar to that of loading (effect size=1.523), at standard temperature, but the improvements were additive in nature (combined effect size=3.032). At thermoneutral temperature, the effect sizes of RAL, loading, and combined were 1.583, 2.813, and 3.655, respectively. The effect size of temperature on its own was small (0.115), further emphasizing the limited impact of temperature. The increase in BV/TV was driven by an increase in trabecular thickness (Tb.Th) and trabecular number (Tb.N), and a decrease in trabecular spacing (Tb.Sp) due to both loading and RAL (Table 1). Thermoneutral temperature decreased trabecular thickness ($p=0.0297$), but again the small effect size (0.033) shows how modest the effect was. A 3-way interaction between temperature, loading, and RAL occurred for tissue mineral density (tTMD, $p=0.0083$) (Fig-2B). Effect sizes reinforced that the contribution from RAL and loading at both standard and thermoneutral temperatures were similar in magnitude. The effects were greater combined than for RAL, loading, or temperature individually. In the case of TMD, the effect size of temperature was larger than for other properties, but still less than RAL and loading at standard temperature and similar to both at thermoneutral temperature.

3.3 Cortical Geometry at the Tibial Mid-Diaphysis is Improved by Loading and RAL Treatment with Modest Impact from Temperature

Cortical bone mass showed effects of loading in all properties investigated. Similar to the trabecular region, there were combined effects of loading and RAL, evident by significant loading x treatment interaction effects, in total area ($p<0.0001$), marrow area ($p=0.0127$), bone area (0.0057), I_{max} ($p=0.0001$), and I_{min} ($p=0.0355$). Loading and RAL both increased each property (Table 3). By assessing the statistical effect sizes of the properties with significant differences, the main contributor to the improvement in geometric properties was loading since the effect sizes are much greater, regardless of the housing temperature. The combined effect sizes for loading and RAL are still greater in most properties, indicating the combination is greater than either single effect (Table 4). Loading and RAL both significantly increased cortical thickness ($p<0.0001$ for both) (Fig-3A). Loading also significantly decreased tissue mineral density (TMD, $p<0.0001$) (Fig-3B). Bone area fraction (BA/TA) was significantly increased by loading ($p<0.0001$) and RAL ($p=0.0021$) and decreased by temperature ($p=0.0022$). Temperature significantly decreased bone area

($p=0.0254$), cortical thickness ($p=0.005$), and I_{\max} ($p=0.0034$), and increased TMD ($p=0.0035$) (Fig-3B). These decreases in properties due to temperature are shown by the negative effect sizes, and the absolute values are smaller than RAL or loading for most properties which verifies the modest impact of temperature compared to the robust loading and treatment responses.

3.4 Temperature Had No Effect on Mechanical Properties or Fracture Toughness Which Were Primarily Impacted by Loading

Four-point bending to failure showed a beneficial effect of loading on both whole bone (ultimate force, failure force, ultimate displacement: all $p<0.0001$, postyield work: $p=0.0241$, and total work: $p=0.0186$) and tissue level (toughness: $p=0.0426$, ultimate stress: $p=0.004$, failure stress: $p=0.0016$, ultimate strain: $p<0.0001$) mechanical properties (Figure 4, Table 5). Treatment impacted fewer mechanical properties. RAL increased ultimate force ($p=0.0092$), stiffness ($p=0.0054$), postyield work ($p=0.0131$), total work ($p=0.0068$), and toughness ($p=0.0393$) and decreased ultimate stress ($p=0.0420$). The statistical effect sizes indicate a greater combination effect between loading and RAL for properties that were increased with RAL treatment. Temperature had no significant effect on any mechanical properties, with small and often negative effect sizes from temperature alone (Supplemental Table S4).

Loading significantly increased the stress intensity factor for crack initiation (Figure 5, $p=0.0012$). There was an interaction effect due to loading x treatment for the stress intensity factor at maximum load. Post-hoc analysis indicated there was only a significant difference between standard: non-loaded, CON vs thermoneutral: loaded, RAL ($p=0.0069$). A loading x treatment interaction effect was present in the stress intensity factor for fracture instability ($p=0.0344$), but there were no significant post-hoc effects. Neither RAL nor temperature had any significant effects on fracture toughness on their own.

4. Conclusion

4.1 Discussion

The novelty of this study was the addition of altered housing temperature to a combined mechanical loading and treatment design. Thermoneutral housing was investigated with the expectation that the removal of cold stress that is imposed upon mice housed at standard temperatures would allow for extra energy that could be utilized towards a response that would accentuate the impacts of loading and raloxifene. Surprisingly, thermoneutral housing failed to have any major effects in either trabecular or cortical architecture and had no positive impact on mechanical properties or fracture resistance. The few effects of temperature which were detected were detrimental to cortical geometry. Temperature impacted the overall size of the bone (bone area, cortical thickness, and I_{\max}) which suggests a delay in growth based expansion. It is interesting to note that aside from these few cortical effects, temperature's only other main effects were to decrease trabecular thickness and decrease body weight. A weight decrease was expected in thermoneutral conditions. A decrease in body weight has been shown with increasing temperature after 26°C in 9 week old mice along with a decrease in BAT tissue weight and other organ weights (heart, liver,

kidneys). The overall loss in body weight at thermoneutral temperatures can most likely be attributed to weight loss in these individual factors. Since BAT tissue is an organ primarily for heat development, it becomes less active when mice are within or closer to their thermoneutral zone. Hypertrophy of the heart and other organs is a well-known phenomenon in acute and long-term exposure to cold temperatures. [1] Nonetheless, the body weight differences between groups were, as mentioned, modest with significance driven by the large sample sizes. If groups are broken up and compared individually (i.e. standard housing CON, standard housing RAL, thermoneutral CON, thermoneutral RAL), the body weight differences between the groups range from 1.7% to 3.5% and all statistical significance is lost. This is one instance that highlights the importance to note that this was a large study with 80 animals, so the modest yet significant changes that were observed due to temperature could have been driven by the high number of samples that were being analyzed. Large sample sizes and the 3-way ANOVA analysis, which pools samples across groups for main effect analyses, may also have boosted the effects of raloxifene as noted below. Mice housed at thermoneutral conditions responded to mechanical loading in almost the same manner as those housed under standard room temperature conditions, indicating that future mechanical loading research in bone can take place at standard temperatures (22°C) if only mechanical or morphological end points are considered. Caution should be taken if end points extend to metabolic measures or gene or protein expression as these may be more sensitive to housing conditions.

Axial compressive loading of the tibia is a common non-invasive external loading modality that has been shown to induce a robust bone formation response in mice. Previous work from our group has shown that a significant 15% increase in cortical thickness is possible after only two weeks of loading female C57BL/6J mice to a maximum tensile strain of 2050 $\mu\epsilon$. [19] By extending the loading duration to 6 weeks, an average cortical thickness increase of 26% was observed at the tibial mid-shaft. [20] The extended 6 week timeframe was chosen for this study to allow time to observe a potential additive effect of loading and RAL, and a metabolic boost from thermoneutral housing was expected. We observed a strong effect on both trabecular architecture and cortical properties due to loading in the current study. There were clear and robust mass-based improvements in each architectural property investigated in both cancellous and cortical regions. The only exception was that cortical tissue mineral density was decreased by loading, while trabecular tissue mineral density was increased. This can likely be explained by the fact that trabecular bone is more sensitive to loading, shows a formation response at lower load levels than cortical locations, and shows a loading formation response earlier and after fewer loading bouts. [19] This could mean that in a 6 week loading study, the trabecular location formed bone first and that new bone would have had extra time to mineralize after forming. In contrast, the formation response took longer to begin at the cortical site and occurred over a longer period of time. Due to the robust response, the new cortical bone that was formed due to loading had less time to mineralize resulting in a lower overall tissue mineral density. Loading clearly increased bone formation because the proximal-mid bone area and cortical thickness increased by 15% and 10% at standard temperatures and 16% and 11% at thermoneutral temperatures, respectively. The increase in thickness was smaller than shown in previous studies, but this could be attributed to the different anatomical location where the properties were determined. [20]

The bone volume fraction in cancellous bone was increased by 26% and 31% in standard and thermoneutral temperatures, respectively. This increase was driven by an increase in trabecular thickness and number and accompanied by a decrease in trabecular spacing. The slightly greater increase in the property at thermoneutral temperatures may indicate a possible metabolic boost in bone formation which we expected to see. However, the difference was minimal and temperature did not have a significant main effect. Overall, housing temperature did not have the pronounced impact on the anabolic effect of loading that was anticipated.

The mass-based improvements due to loading translated to increased whole bone mechanical properties. Loading shifted the force-displacement curve up which increased the maximum and failure forces and also increased the postyield work and total work. The improvements to postyield work and total work were more modest compared to the other loading effects, but this could be attributed to the higher variability in post-yield properties. [30] Not only were ultimate and failure forces increased, but so were the corresponding stresses which indicates improvements were not solely mass-based and perhaps tissue quality was also improved. Similarly to total work, toughness was improved but was a more modest change. Fracture toughness is a more direct measure of the tissue behavior and fracture resistance since it tests the ability of the tissue to resist the initiation and propagation of a defined crack. The increase in crack initiation and maximum load stress intensity factors with loading are further indicators of improved bone tissue quality. The lack of interactions between loading and temperature indicate that thermoneutrality does not alter the anabolic response to loading and impacts on bone mechanics.

Raloxifene is known to control bone resorption by binding to osteoblasts and activating the estrogen receptor. Other non-cellular mechanisms have been demonstrated to improve tissue quality which could explain how the drug is capable of reducing fracture risk in osteoporosis patients. [10] Raloxifene's ability to improve tissue quality could be amplified and reflected in architectural and mechanical improvements if administered during an active bone formation response. Previous work from our group demonstrated combination effects of loading and raloxifene in female mice, but the effects were less pronounced than predicted. [20] The current study displayed similar effects, providing further support for the potential of combination treatments for advanced improvements. In this case, loading drove most improvements, yet raloxifene still improved both cancellous and cortical architecture. Raloxifene improved every property investigated in cancellous bone, but the effects in cortical bone were more modest as shown by the smaller effect sizes. Interestingly, there were several treatment and temperature interactions that occurred in cancellous bone. This is in line with other work that has shown improvements in cancellous bone, but not cortical bone. However, the effect sizes of temperature were small for trabecular properties. Large sample sizes and the power that comes with the 3-way ANOVA analysis may be the explanation for the boosted effects of raloxifene that were seen compared to previous work. Treatment had a more modest impact on bone mechanics. Elastic modulus was increased by raloxifene treatment and this, along with other mechanical properties, was a modest change (quantified by a small effect size) that may be attributed to the large sample sizes and requires further investigation.

4.2 Limitations and Future Work

This study showed that housing temperature had limited effect on bone morphology or mechanical properties when mice were subjected to either mechanical loading or pharmaceutical treatment, yet other studies with thermoneutral housing in mice have shown greater effects. One study demonstrated that thermoneutral housing (32°C) prevented premature cancellous bone loss in female C57BL/6J mice. The mechanisms mediating premature bone loss are not well established, however, C57BL/6J mice housed at thermoneutral temperature did not exhibit the cancellous bone loss in distal femur that is typically noted in standard temperature-housed mice, suggesting housing temperature is a critical factor. [3,4] This study was investigating bone loss and was, therefore, much longer than ours (14 weeks for the C57Bl/6 mouse model and 18 weeks for the C3H mouse model vs our 6 week study). The bone loss that occurs from 8 weeks of age (peak cancellous bone mass) until the age of 18–22 weeks (peak bone mass) is significant and could offer a greater opportunity for the metabolic boost that we were expecting to see in our study to actually have an effect and improve architecture. Interestingly, this group did not observe any robust differences in bone length or cortical architecture, similar to our study. Other work in osteoporotic mice also showed improved trabecular bone without improvements in cortical bone in mice exposed to higher housing temperatures. [5] The mass-based trabecular improvements translated to mechanical improvements in the yield point and ultimate force in the femur as tested in three-point bending. Main differences between this study and the current study are the disease state model, higher temperature housing (34°C), and older mice (16 weeks to 24 weeks). It seems that the osteoporotic model provides another opportunity for the extra energy that is being conserved in thermoneutral conditions to be utilized towards an improved response. Future work in different ages, disease models, and organ systems may be necessary to extend the findings of this study.

There were other limitations to the current study. Female mice were chosen intentionally due to the clinical relevance of raloxifene treatment, however, in future studies it may be important to assess the impact of housing temperature on both sexes. A strain calibration was run prior to the study to determine the maximum load necessary to induce a tensile strain of 2050 $\mu\epsilon$. Loading to the same maximum load throughout the 6 week study assumes that the strain stays constant, but strain would change as the bone changes with loading, treatment, and age so that the different groups would eventually see different strains when loading to the same force. Future studies may need to include a second strain calibration on a subset of mice from each group during the study to adjust load levels. This study was also lacking in a mechanistic exploration for changes (or lack thereof) in bone due to thermoneutral housing. Investigating mechanism was not in the scope of the original study design and given the fact that little impact of thermoneutrality was noted, it was decided not to pursue these effects.

In summary, combined effects of external loading and raloxifene on bone morphology and mechanical properties were demonstrated. Thermoneutral housing failed to increase these effects. Future work will aim to consider the effect of thermoneutral housing in disease states so that the temperature may provide that metabolic boost that was expected to further enhance the combined effect of loading and raloxifene.

Supplementary Material

Refer to Web version on PubMed Central for supplementary material.

Acknowledgements

This work was supported by the National Institutes of Health [AR072609]. The authors would like to acknowledge the Integrated Nanosystems Development Institute (INDI) for use of their JEOL7800F Field Emission Scanning Electron Microscope, which was awarded through NSF grant MRI-1229514.

References

- Gordon CJ, "Thermal physiology of laboratory mice: Defining thermoneutrality," *Journal of Thermal Biology*, vol. 37, pp. 654–85, 2012.
- Claire Hankenson F, Marx JO, Gordon CJ, and David JM, "Effects of Rodent Thermoregulation on Animal Models in the Research Environment," *Comparative Medicine*, vol. 68 (6), pp. 425–38, 2018. [PubMed: 30458902]
- Iwaniec UT, Philbrick KA, Wong CP, Gordon JL, Kahler-Quesada AM, Olson DA, Branscum AJ, Sargent JL, DeMambro VE, Rosen CJ, and Turner RT, "Room temperature housing results in premature cancellous bone loss in growing female mice: implications for the mouse as a preclinical model for age-related bone loss," *Osteoporosis Int*, vol. 27, pp. 3091–3101, 2016.
- Martin SA, Philbrick KA, Wong CP, Olsen DA, Branscum AJ, Jump DB, Marik CK, DenHerder JM, Sargent JL, Turner RT, and Iwaniec UT, "Thermoneutral housing attenuates premature cancellous bone loss in male C57BL/6J mice," *Endocrine Connections*, vol. 8, no. 11, pp. 1455–67, 2019. [PubMed: 31590144]
- Chevalier C et al., "Warmth Prevents Bone Loss Through the Gut Microbiota," *Cell Metabolism*, vol. 32, pp. 1–16, 2020. [PubMed: 32589948] Taranta A, Brama M, Teti A, Scandurra R, Spera G, Agnusdei D, et al., "The selective estrogen receptor modulator raloxifene regulates osteoclast and osteoblast activity in vitro," *Bone*, vol. 30, pp. 368–76, 2002. [PubMed: 11856644]
- Bryant HU, Mechanism of action and preclinical profile of raloxifene, a selective estrogen receptor modulation," *Rev Endocr Metab Disord*, vol. 2, no. 1, pp. 129–38, 1 2001. [PubMed: 11704975]
- Ettinger B, Black DM, Mitlak BH, Knickerbocker RK, Nickelsen T, Genant HK, Christiansen C, Delmas PD, Zanchetta JR, Stakkestad J, Gluer CC, Krueger K, Cohen FJ, Eckert S, Ensrud KE, Avioli LV, Lips P, and Cummings SR, "Reduction of vertebral fracture risk in postmenopausal women with osteoporosis treated with raloxifene: results from a 3-year randomized clinical trial," *JAMA*, vol. 282, no. 7, pp. 637–45, 1999. [PubMed: 10517716]
- Seeman E, Crans GG, Diez-Perez A, Pinette KV, and Delmas PD, "Anti-vertebral fracture efficacy of raloxifene: a meta-analysis," *Osteoporosis international*, vol 17, pp. 313–16, 2006. [PubMed: 16217588]
- Bivi N, Hu H, Chavali B, Chalmers MJ, Reutter CT, Durst GL, et al., "Structural features underlying raloxifene's biophysical interaction with bone matrix," *Bioorganic & medicinal chemistry*, vol. 24, pp. 759–67, 2016. [PubMed: 26795112]
- Gallant MA, M Brown D, Hammond M, Wallace JM, Du J, Deymier-Black AC, et al., "Bone cell-independent benefits of raloxifene on the skeleton: a novel mechanism for improving bone material properties," *Bone*, vol. 61, pp. 191–200, 2014. [PubMed: 24468719]
- Allen MR, Aref MW, Newman CL, Kadakia JR, and Wallace JM, "El Raloxifeno invierte fragilidad Ósea inducida por el tratamiento anti-remodelación y aumenta la resistencia a la fatiga a través de mecanismos mediados no celulares," *Actualizaciones en Osteología*, vol. 12, pp. 169–179, 2016.
- Burr DB and Akkus O, Chapter 11 – Mechanical Adaptation. San Diego: Academic Press, 2014, pp. 206–9.
- Dalen N and Olsson KE, "Bone mineral content and physical activity," *Acta Orthop Scand*, vol. 45, pp. 170–4, 1974. [PubMed: 4406972]

14. Wolman RL, Faulmann L, Clark P, Hesp R, and Harries MG, “Different training patterns and bone mineral density of the femoral shaft in elite, female athletes,” *Ann Rheum Dis*, col. 50, pp. 487–9, 1991.
15. Fuchs RK, Bauer JJ, and Snow CM, “Jumping improves hip and lumbar spine bone mass in prepubescent children: a randomized controlled trial,” *J Bone Miner Res*, vol. 16, pp. 148–56, 2001. [PubMed: 11149479]
16. De Souza RL, Matsuura M, Eckstein F, Rawlinson SC, Lanyon LE, and Pitsillides AA, “Noninvasive axial loading of mouse tibiae increases cortical bone formation and modifies trabecular organization: a new model to study cortical and cancellous compartments in a single loaded element,” *Bone*, vol. 37, pp. 810–8, 2005. [PubMed: 16198164]
17. Fritton JC, Myers ER, Wright TM, and van der Meulen MCH, “Loading induces site specific increases in mineral content assessed by microcomputed tomography of the mouse tibia,” *Bone* vol. 36, pp. 1030–8, 2005. [PubMed: 15878316]
18. Weatherholt AM, Fuchs RK, and Warden SJ, “Cortical and trabecular bone adaptation to incremental load magnitudes using the mouse tibial axial compression loading model,” *Bone*, vol. 52, pp. 372–9, 2013. [PubMed: 23111313]
19. Berman A, Clauser C, Wunderlin C, Hammond MA, Wallace JM, “Structural and Mechanical Improvements to Bone are Strain Dependent with Axial Compression of the Tibia in Female C57BL/6 Mice,” *PloS One*, vol. 10, no. 6, p. e0130504, 2015. [PubMed: 26114891]
20. Berman AG, Damrath JD, Hatch J, Pulliam AN, Powell KM, Hinton M, Wallace JM, “Effects of Raloxifene and Targeted Tibial Loading on Bone Mass and Mechanics in Male and Female Mice,” *Connective Tissue Research* 2021. Online ahead of print.
21. Allen MR, Hogan HA, Hobbs WA, Koivuniemi AS, Koivuniemi MC, and Burr DB, “Raloxifene enhances material-level mechanical properties of femoral cortical and trabecular bone,” *Endocrinology*, vol. 148, no. 8, pp. 3908–13, 2007. [PubMed: 17478550]
22. Allen MR, Territo PR, Lin C, Persohn S, Jiang L, Riley AA, McCarthy BP, Newman CL, Burr DB, and Hutchins GD, “In vivo ute-mri reveals positive effects of raloxifene on skeletal-bound water in skeletally mature beagle dogs,” *J Bone Miner Res*, vol. 30, no. 8, pp. 1441–4, 2015. [PubMed: 25644867]
23. Berman AG, Wallace JM, Bart ZR, and Allen MR, “Raloxifene reduces skeletal fractures in an animal model of osteogenesis imperfecta,” *Matrix Biol*, vol. 52–54, pp. 19–28, 2016.
24. Larsen R, Peveler J, Klutke J, Hickman D, Aref MW, Wallace JM, Brown D, Allen MR, “Effects of daily restraint with and without injections on skeletal properties in C57BL/6NHsd mice,” *Lab Animal*, vol. 46, no. 7, pp. 299–301, 2017. [PubMed: 28644445]
25. Sugiyama T, Price JS and Lanyon LE, “Functional adaptation to mechanical loading in both cortical and cancellous bone is controlled locally and is confined to the loaded bones,” *Bone*, vol. 46, no. 2, pp. 314–321, 2010. [PubMed: 19733269]
26. Berman A, Hinton MJ, and Wallace JM, “Treadmill running and targeted tibial loading differentially improve bone mass in mice,” *Bone reports*. 2019;10:100195. [PubMed: 30701187]
27. Wallace JM, Golcuk K, Morris MD, and Kohn DH, “Inbred strain-specific response to biglycan deficiency in the cortical bone of C57BL6/129 and C3H/He mice,” *J Bone Miner Res*, vol. 24, no. 6, pp. 1002–12, 2009. [PubMed: 19113913]
28. Ritchie RO, Koester KJ, Ionova S, Yao W, Lane NE, and r. Ager JW, “Measurement of the toughness of bone: a tutorial with special reference to small animal studies,” *Bone*, vol. 43, no. 5, pp. 798–812, 2008. [PubMed: 18647665]
29. Hammond MA, Berman AG, Pacheco-Costa R, Davis HM, Plotkin LI, and Wallace JM, “Removing or truncating connexin 43 in murine osteocytes alters cortical geometry, nanoscale morphology, and tissue mechanics in the tibia,” *Bone*, vol. 88, pp. 85–91, 2016. [PubMed: 27113527]
30. Currey JD, Pitchford JW, and Baxter PD, “Variability of the mechanical properties of bone, and its evolutionary consequences,” *J R Society*, vol. 4, no. 12, pp. 127–135, 2007.

Highlights:

- Thermal physiological characteristics of mice can impact research outcomes.
- Thermoneutrality was superimposed on tibial compression and Raloxifene treatment.
- Temperature modestly impacted weight and bone architecture, often detrimentally.
- Thermoneutrality had no impact on mechanical integrity.
- Raloxifene and loading resulted in additive improvements in bone properties.

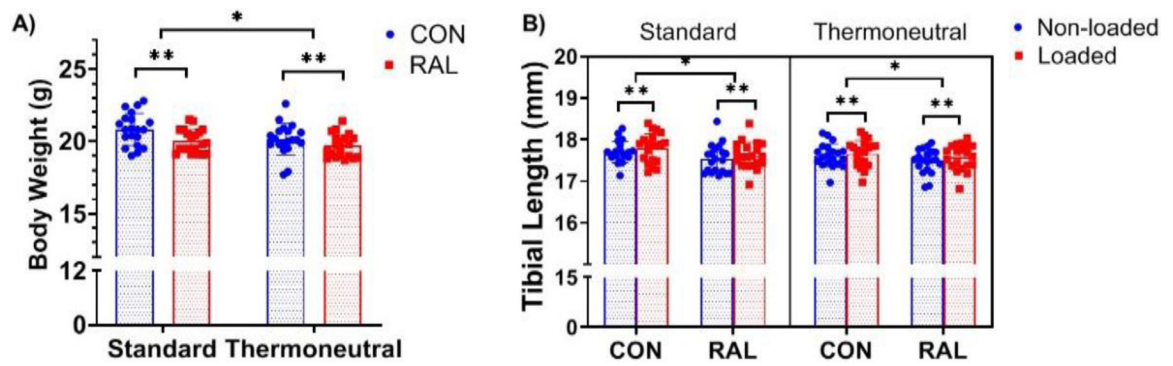


Figure 1.

n=20 for each group. **A)** Final body weights (n=20) decreased with temperature and RAL

treatment. 2-way ANOVA performed with main effects of treatment and temperature: **

p=0.004, * p=0.0196. **B)** Left tibiae (loaded) were longer than right tibiae (non-loaded). 3-

way ANOVA performed with main effects of temperature, loading, and treatment. **

p=0.0022, * p=0.0306.

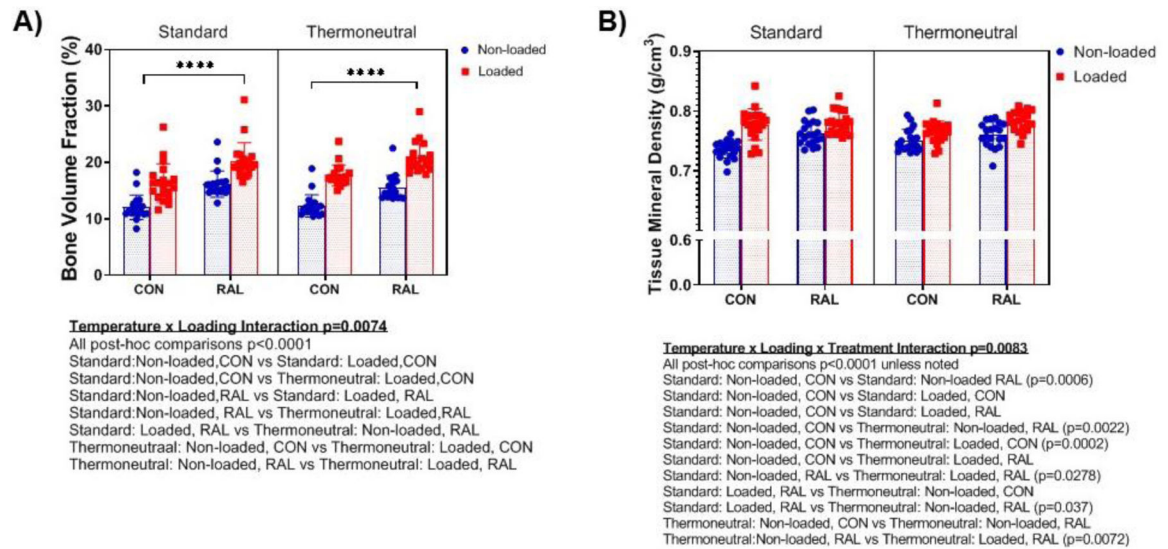


Figure 2.
 Trabecular geometry of right (non-loaded) and left (loaded) tibiae ($n=20$ per group). **A)** Bone volume fraction increased significantly due to RAL treatment. **B)** A three way interaction effect occurred for tissue mineral density. **** $p<0.0001$.

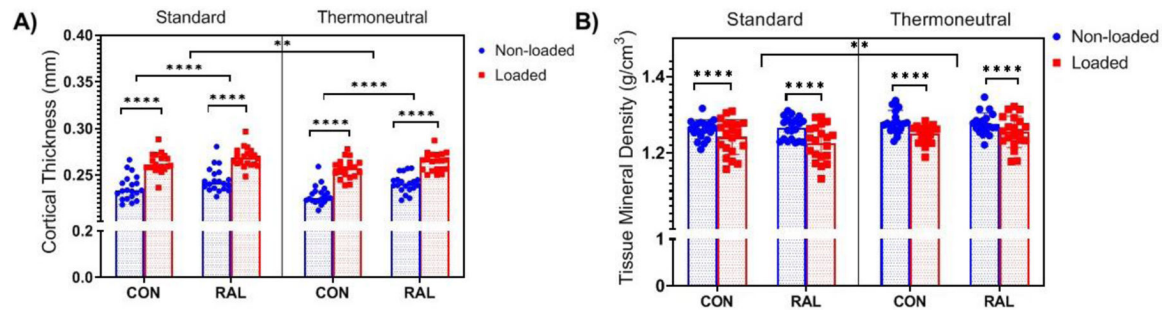


Figure 3.

Cortical properties of right (non-loaded) and left (loaded) tibiae (n=20 per group). **A)**

Cortical thickness was increased due to loading and RAL and decreased due to temperature.

**** p<0.0001, ** p=0.005. **B)** Tissue mineral density was decreased due to loading and increased due to temperature. **** p<0.0001, ** p=0.0035.

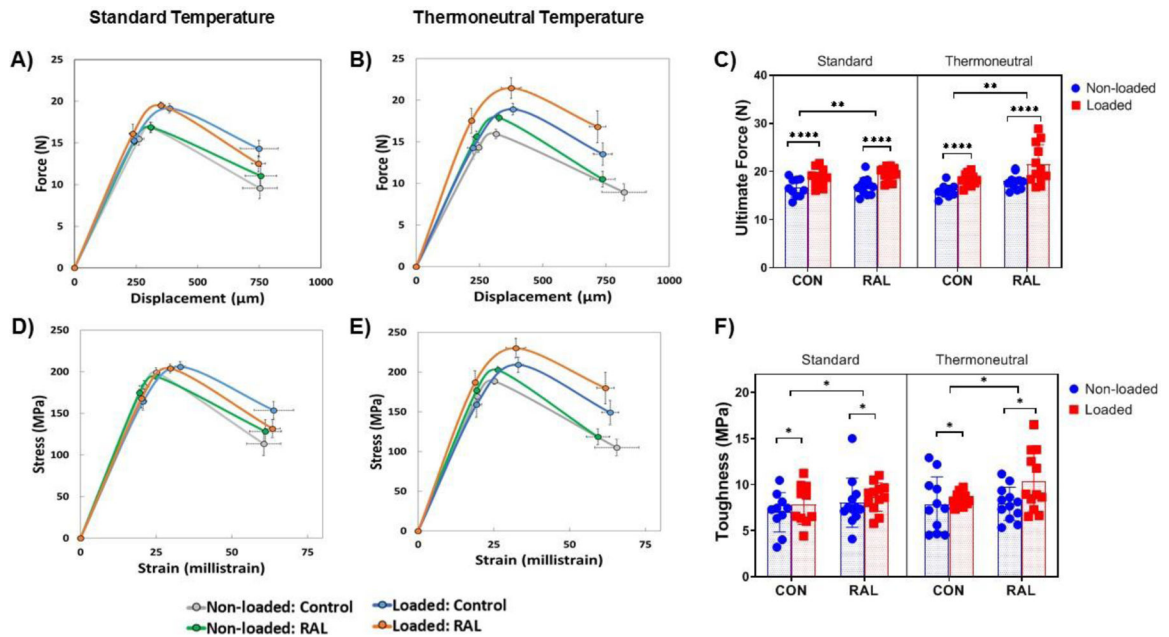


Figure 4.

Mechanical properties of right and left tibiae; standard-CON (n=10), standard-RAL (n=12), thermoneutral-CON (n=11), thermoneutral-RAL (n=12). **A)** Average force-displacement plot for standard temperature, showing stronger loaded bones (mean \pm SEM). **B)** The strength disparity continued at the thermoneutral temperature as quantified by **C)** the ultimate force. **D)** Average stress-strain plots for mice housed at standard temperature show how tissue-level properties increase with loading and RAL, **E)** with similar results at thermoneutral temperature. **F)** Bone toughness increases with loading and RAL treatment. **** $p < 0.0001$, ** $p = 0.0092$, * $p = 0.05$.

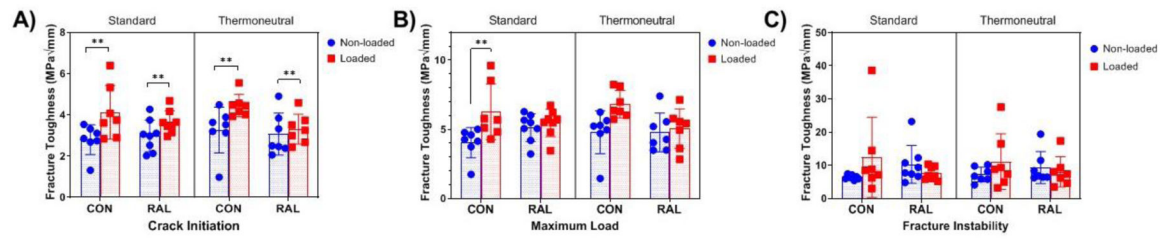


Figure 5. Fracture toughness stress intensity factors for **A)** crack initiation, **B)** maximum load, and **C)** fracture instability. Loading increased crack initiation (** p=0.0012) and thermoneutral: loaded, CON increased from standard: non-loaded, CON (p=0.0069).

Table 1.

Trabecular properties of right (non-loaded) and left (loaded) tibiae (n=20 per group). RM 3-way ANOVA test with temperature (temp), loading (load), and treatment (treat) main effects.

	Standard						Thermonutral						P-value						
	Non-loaded		Loaded		Non-loaded		Loaded		Non-loaded		Loaded		Temperature	Loading	Treatment	Temperature * Loading	Temperature * Treatment	Loading * Treatment	Temperature * Loading * Treatment
	Control	RAL	Control	RAL	Control	RAL	Control	RAL	Control	RAL	Control	RAL							
BV/T V (%)	12 ± 2.1	16.2 ± 2.3	16.4 ± 3.4	20.3 ± 3.2	12.3 ± 2	15.5 ± 2.1	17.7 ± 1.9	20.8 ± 2.6	12.3 ± 2	15.5 ± 2.1	17.7 ± 1.9	20.8 ± 2.6	0.5026	<0.0001	<0.0001	0.0074	0.4264	0.6676	0.9690
Tb.Th (µm)	6.14 ± 0.21	6.73 ± 0.26	7.68 ± 0.71	7.91 ± 0.42	6.14 ± 0.19	6.61 ± 0.2	7.39 ± 0.31	7.82 ± 0.3	6.14 ± 0.19	6.61 ± 0.2	7.39 ± 0.31	7.82 ± 0.3	0.0297	<0.0001	<0.0001	0.2884	0.7485	0.0937	0.1595
Tb.Sp (µm)	23.66 ± 1.98	22.68 ± 1.51	23.1 ± 2.85	21.55 ± 1.65	23.58 ± 1.67	22.23 ± 1.68	21.52 ± 1.7	21.27 ± 1.93	23.58 ± 1.67	22.23 ± 1.68	21.52 ± 1.7	21.27 ± 1.93	0.1352	<0.0001	0.0107	0.0465	0.5541	0.4041	0.0129
Tb.N (1/ µm)	0.02 ± 0	0.02 ± 0	0.02 ± 0	0.03 ± 0	0.02 ± 0	0.02 ± 0	0.02 ± 0	0.03 ± 0	0.02 ± 0	0.02 ± 0	0.02 ± 0	0.03 ± 0	0.2550	<0.0001	<0.0001	0.0003	0.4093	0.3230	0.3968
TMD (g/ cm ³)	0.74 ± 0.01	0.76 ± 0.02	0.78 ± 0.03	0.78 ± 0.02	0.75 ± 0.02	0.76 ± 0.02	0.76 ± 0.02	0.78 ± 0.02	0.75 ± 0.02	0.76 ± 0.02	0.76 ± 0.02	0.78 ± 0.02	0.8218	<0.0001	<0.0001	0.0615	0.8950	0.1820	0.0083

Trabecular effect sizes are much smaller for temperature than either RAL treatment or loading indicating the modest effect that thermoneutral housing had on trabecular geometry.

Table 2.

Geometric Property	Standard Temperature			Thermoneutral Temperature			Temp effect
	RAL	Loading	Combined	RAL	Loading	Combined	
BV/TV	1.837	1.523	3.032	1.583	2.813	3.655	0.115
Tb.Th	2.524	2.944	5.362	2.391	4.899	6.662	0.033
Tb.Sp	-0.562	-0.232	-1.163	-0.808	-1.225	-1.278	-0.045
Tb.N	1.271	0.420	1.672	1.101	1.250	1.957	0.099
TMD	1.551	1.939	2.623	0.517	0.772	1.849	0.886

Table 3.

Cortical properties of right (non-loaded) and left (loaded) tibiae (n=20 per group).

	Non-loaded		Loaded		Non-loaded		Loaded		Temperature	Loading	Treatment	Temperature * Loading	Temperature * Treatment	Loading * Treatment	Temperature * Loading * Treatment
	Control	RAL	Control	RAL	Control	RAL	Control	RAL							
Total area (mm ²)	1.26 ± 0.07	1.3 ± 0.07	1.43 ± 0.06	1.43 ± 0.05	1.24 ± 0.06	1.32 ± 0.05	1.41 ± 0.05	1.43 ± 0.04	0.6868	<0.0001	0.0043	0.4527	0.2365	<0.0001	0.5296
Marrow Area (mm ²)	0.49 ± 0.03	0.49 ± 0.03	0.52 ± 0.05	0.5 ± 0.03	0.5 ± 0.03	0.51 ± 0.04	0.52 ± 0.04	0.52 ± 0.03	0.0780	<0.0001	0.8589	0.3645	0.3602	0.0127	0.9386
Bone Area (mm ²)	0.77 ± 0.06	0.81 ± 0.05	0.91 ± 0.03	0.93 ± 0.04	0.75 ± 0.04	0.81 ± 0.03	0.89 ± 0.04	0.91 ± 0.03	0.0254	<0.0001	<0.0001	0.9864	0.3358	0.0057	0.4614
Bone Area Fraction (%)	61.36 ± 1.87	62.37 ± 1.97	63.69 ± 2.15	64.94 ± 1.7	60.02 ± 1.7	61.18 ± 2.25	63.02 ± 1.88	63.89 ± 1.61	0.0022	<0.0001	0.0021	0.4424	0.8679	0.9651	0.6203
Cortical Thickness (mm)	0.24 ± 0.01	0.24 ± 0.01	0.26 ± 0.01	0.27 ± 0.01	0.23 ± 0.01	0.24 ± 0.01	0.26 ± 0.01	0.26 ± 0.01	0.005	<0.0001	<0.0001	0.8663	0.5172	0.1900	0.6031
Imax (mm ⁴)	0.2 ± 0.03	0.22 ± 0.03	0.27 ± 0.03	0.27 ± 0.02	0.18 ± 0.02	0.21 ± 0.01	0.26 ± 0.02	0.26 ± 0.02	0.0034	<0.0001	0.0585	0.7573	0.6017	0.0001	0.3859
Imin (mm ⁴)	0.07 ± 0.01	0.08 ± 0.01	0.11 ± 0.01	0.11 ± 0.01	0.07 ± 0.01	0.08 ± 0.01	0.09 ± 0.01	0.1 ± 0.01	0.5483	<0.0001	0.0007	0.3130	0.1056	0.0355	0.9326
TMD (g/cm ³ HA)	1.26 ± 0.03	1.26 ± 0.03	1.24 ± 0.05	1.23 ± 0.05	1.28 ± 0.03	1.28 ± 0.03	1.25 ± 0.02	1.26 ± 0.04	0.0035	<0.0001	0.5888	0.8199	0.6075	0.7421	0.1712

Temperature effect sizes are negative for nearly all cortical properties and the absolute values are less than most RAL and loading effect sizes suggesting a modest impact.

Table 4.

Geometric Property	Effect Sizes							
	Standard Temperature			Thermonutral Temperature			Temp effect	
	RAL	Loading	Combined	RAL	Loading	Combined		
Total Area	0.601	2.577	2.783	1.36	3.005	3.777		-0.277
Marrow Area	0.090	0.817	0.451	0.394	0.715	0.647		0.319
Bone Area	0.721	2.994	3.297	1.701	3.671	4.618		-0.581
Bone Area Fraction	0.523	1.155	1.998	0.579	1.671	2.339		-0.750
Cortical Thickness	0.656	2.200	2.738	1.271	2.759	3.537		-0.674
Imax	0.480	2.404	2.632	1.225	3.489	3.311		-0.743
Imin	0.535	2.448	2.536	1.247	2.511	3.739		-0.118
TMD	0.115	-0.543	-0.937	0.198	-1.209	-0.744		0.739

Table 5.

Mechanical properties of right (non-loaded) and left (loaded) tibiae.

	Structural Mechanical Properties from 4-point bending										RM 3 Way ANOVA														
	Standard		Thermonutral				RM 3 Way ANOVA				Temperature			Temperature x Loading			Temperature x Treatment			Loading x Treatment			Temperature x Loading x Treatment		
	Non-loaded	Loaded	Control	RAL	Control	RAL	Control	RAL	Control	RAL	Temperature	Loading	Treatment	Temperature x Loading	Temperature x Treatment	Loading x Treatment	Temperature x Loading x Treatment								
Yield Force (N)	15.5 ± 2.6	15.3 ± 3.5	16.1 ± 3.8	14.3 ± 2.1	14.3 ± 4.7	17.5 ± 5	14.3 ± 2.1	14.3 ± 4.7	17.5 ± 5	0.8146	0.2374	0.1086	0.7089	0.1391	0.3136	0.2580									
Ultimate Force (N)	16.8 ± 2.2	19.1 ± 1.8	19.5 ± 1.4	15.9 ± 2	18.9 ± 2.4	21.5 ± 4.1	17.9 ± 1.5	18.9 ± 2.4	21.5 ± 4.1	0.2873	<0.0001	0.0092	0.6309	0.7800	0.1391	0.3136									
Failure Force (N)	9.6 ± 4.3	14.3 ± 3.5	12.5 ± 3.2	8.9 ± 3.6	13.5 ± 4.7	16.8 ± 6.4	10.5 ± 3.2	13.5 ± 4.7	16.8 ± 6.4	0.6454	<0.0001	0.2081	0.2637	0.1076	0.9538	0.1134									
Ultimate Displacement (µm)	310.5 ± 53.3	386 ± 64.4	350.7 ± 59.3	315.7 ± 22.1	382.3 ± 62.6	376 ± 130.4	326.8 ± 30.2	382.3 ± 62.6	376 ± 130.4	0.2352	<0.0001	0.7738	0.8310	0.7527	0.2484	0.6022									
Displacement to Yield (µm)	261.4 ± 71.5	242.2 ± 47.4	237.4 ± 49.8	246.4 ± 33	224.2 ± 71.9	217.8 ± 25.6	239.1 ± 20.1	224.2 ± 71.9	217.8 ± 25.6	0.2256	0.4245	0.3548	0.1786	0.9043	0.5484	0.6713									
Postyield Displacement (µm)	490.8 ± 250.9	506.8 ± 286.6	509.7 ± 100.3	574.8 ± 297.9	513.4 ± 120.4	498.7 ± 108.4	497.5 ± 170	513.4 ± 120.4	498.7 ± 108.4	0.3671	0.3789	0.7537	0.9567	0.2131	0.4065	0.9806									
Total Displacement (µm)	752.2 ± 242.4	749 ± 267.5	747.1 ± 91.3	821.2 ± 304.3	737.6 ± 127.8	716.5 ± 106.2	736.6 ± 163	737.6 ± 127.8	716.5 ± 106.2	0.4975	0.3098	0.8971	0.8134	0.1900	0.5002	0.9096									
Stiffness (N/mm)	67.5 ± 10.8	70.2 ± 9.9	75.7 ± 10.7	65.6 ± 10.9	73 ± 17.9	91.7 ± 29.3	73.1 ± 7.3	73 ± 17.9	91.7 ± 29.3	0.2950	0.0476	0.0054	0.1711	0.0734	0.0631	0.2978									
Work to Yield (mJ)	2.2 ± 1	2 ± 0.8	2.1 ± 0.9	1.9 ± 0.5	1.8 ± 0.9	2 ± 0.6	2 ± 0.4	1.8 ± 0.9	2 ± 0.6	0.5247	0.4947	0.7883	0.3055	0.5615	0.9155	0.6343									
Postyield Work (mJ)	5.4 ± 2.3	7.9 ± 4.5	7.6 ± 1.4	6.1 ± 2.7	7.7 ± 2.5	9.1 ± 3.4	6.7 ± 2	7.7 ± 2.5	9.1 ± 3.4	0.1129	0.0241	0.0131	0.5530	0.9781	0.4868	0.4168									
Total Work (mJ)	7.6 ± 2.2	9.9 ± 4.1	9.7 ± 1.3	8 ± 0	9.5 ± 2.3	11.1 ± 3.5	8.7 ± 2	9.5 ± 2.3	11.1 ± 3.5	0.1323	0.0186	0.0068	0.7360	0.8834	0.4816	0.3661									
Estimated Tissue-Level Mechanical Properties from 4-point bending																									
	Standard				Thermonutral				RM 3 Way ANOVA				Temperature												
	Non-loaded		Loaded		Non-loaded		Loaded		Temperature		Loading		Treatment		Temperature x Loading		Temperature x Treatment		Loading x Treatment		Temperature x Loading x Treatment				
	Control	RAL	Control	RAL	Control	RAL	Control	RAL	Temperature	Loading	Treatment	Temperature x Loading	Temperature x Treatment	Loading x Treatment	Temperature x Loading x Treatment										

Structural Mechanical Properties from 4-point bending																										
	Standard						Thermoneutral						RM 3 Way ANOVA													
	Non-loaded		Loaded		Non-loaded		Loaded		Non-loaded		Loaded		Temperature		Loading		Treatment		Temperature x Loading		Temperature x Treatment		Loading x Treatment		Temperature x Loading x Treatment	
	Control	RAL	Control	RAL	Control	RAL	Control	RAL	Control	RAL	Control	RAL	Control	RAL	Control	RAL	Control	RAL	Control	RAL	Control	RAL	Control	RAL	Control	RAL
Yield Stress (MPa)	182.5 ± 23.9	174.8 ± 13	164.2 ± 36	167.7 ± 38.3	169.5 ± 18.7	176.9 ± 23	159 ± 54.8	187.2 ± 48.3	176.9 ± 23	169.5 ± 18.7	176.9 ± 23	159 ± 54.8	187.2 ± 48.3	0.8880	0.4435	0.2805	0.8931	0.1219	0.3149	0.2542						
Ultimate Stress (MPa)	199.1 ± 19.2	194.3 ± 18.7	206 ± 21.1	203.9 ± 17.3	188.6 ± 14.2	202.5 ± 14.9	209.1 ± 33.4	230.1 ± 41.2	202.5 ± 14.9	188.6 ± 14.2	202.5 ± 14.9	209.1 ± 33.4	230.1 ± 41.2	0.1577	0.0040	0.0420	0.1963	0.0369	0.1888	0.4190						
Failure Stress (MPa)	113.4 ± 48.6	128.2 ± 47.1	153.6 ± 36.7	131.5 ± 35.8	104.9 ± 36.6	118.4 ± 33.6	149 ± 53.3	179.8 ± 66.3	118.4 ± 33.6	104.9 ± 36.6	118.4 ± 33.6	149 ± 53.3	179.8 ± 66.3	0.6870	0.0016	0.2987	0.1727	0.1084	0.9337	0.1240						
Ultimate Strain (me)	25 ± 4.2	25 ± 1.7	33 ± 5.5	29.7 ± 4.8	25.2 ± 2.5	26.4 ± 2.4	33 ± 6	32.3 ± 10.7	26.4 ± 2.4	25.2 ± 2.5	26.4 ± 2.4	33 ± 6	32.3 ± 10.7	0.1782	< 0.0001	0.6817	0.9632	0.7153	0.2115	0.6372						
Strain to Yield (me)	21 ± 5.6	19.5 ± 1.9	20.7 ± 4	20.2 ± 4.6	19.6 ± 0	19.3 ± 1.7	19.3 ± 6	18.8 ± 2.5	19.3 ± 1.7	19.6 ± 0	19.3 ± 1.7	19.3 ± 6	18.8 ± 2.5	0.2632	0.3884	0.3821	0.2338	0.9885	0.4926	0.6921						
Total Strain (me)	60.5 ± 19.5	61.1 ± 17.3	63.8 ± 22.4	63.4 ± 8.4	65.6 ± 25.2	59.3 ± 12.7	63.4 ± 9.6	61.9 ± 9.5	59.3 ± 12.7	65.6 ± 25.2	59.3 ± 12.7	63.4 ± 9.6	61.9 ± 9.5	0.4144	0.9729	0.8663	0.9224	0.1830	0.5205	0.9031						
Modulus (GPa)	9.9 ± 1.3	10.2 ± 1.4	8.8 ± 1.2	9.3 ± 1.2	9.7 ± 0.8	10.3 ± 0.9	9.4 ± 2.6	11.3 ± 3.3	10.3 ± 0.9	9.7 ± 0.8	10.3 ± 0.9	9.4 ± 2.6	11.3 ± 3.3	0.2525	0.0894	0.0059	0.0961	0.0234	0.0412	0.3124						
Resilience (MPa)	2.1 ± 0.9	1.8 ± 0.2	1.9 ± 0.7	1.9 ± 0.8	1.8 ± 0.4	1.8 ± 0.4	1.7 ± 0.9	1.9 ± 0.5	1.8 ± 0.4	1.8 ± 0.4	1.8 ± 0.4	1.7 ± 0.9	1.9 ± 0.5	0.6434	0.6345	0.9011	0.5419	0.5535	0.9409	0.6230						
Toughness (MPa)	7.3 ± 2.1	8 ± 2.7	9.1 ± 3.8	8.6 ± 1.5	7.7 ± 2.9	7.9 ± 1.8	9.1 ± 2.4	10.3 ± 3.3	7.9 ± 1.8	7.7 ± 2.9	7.9 ± 1.8	9.1 ± 2.4	10.3 ± 3.3	0.1043	0.0426	0.0393	0.4952	0.9069	0.4574	0.3247						